



**UNIVERSITY OF LEEDS**

This is a repository copy of *Coupled Calculations of Bubble Departure Diameter and Frequency from Mechanistic Principles for Nucleate Boiling Applications*.

White Rose Research Online URL for this paper:  
<http://eprints.whiterose.ac.uk/152048/>

Version: Accepted Version

---

**Proceedings Paper:**

Colombo, M and Fairweather, M (2019) Coupled Calculations of Bubble Departure Diameter and Frequency from Mechanistic Principles for Nucleate Boiling Applications. In: Proceedings of 18th International Topical Meeting on Nuclear Reactor Thermal Hydraulics (NURETH-18). 18th International Topical Meeting on Nuclear Reactor Thermal Hydraulics (NURETH-18), 18-23 Aug 2019, Portland, USA. .

---

**Reuse**

Items deposited in White Rose Research Online are protected by copyright, with all rights reserved unless indicated otherwise. They may be downloaded and/or printed for private study, or other acts as permitted by national copyright laws. The publisher or other rights holders may allow further reproduction and re-use of the full text version. This is indicated by the licence information on the White Rose Research Online record for the item.

**Takedown**

If you consider content in White Rose Research Online to be in breach of UK law, please notify us by emailing [eprints@whiterose.ac.uk](mailto:eprints@whiterose.ac.uk) including the URL of the record and the reason for the withdrawal request.



[eprints@whiterose.ac.uk](mailto:eprints@whiterose.ac.uk)  
<https://eprints.whiterose.ac.uk/>

# **COUPLED CALCULATIONS OF BUBBLE DEPARTURE DIAMETER AND FREQUENCY FROM MECHANISTIC PRINCIPLES FOR NUCLEATE BOILING APPLICATIONS**

**Marco Colombo and Michael Fairweather**

School of Chemical and Process Engineering, University of Leeds,  
Leeds LS2 9JT, United Kingdom  
M.Colombo@leeds.ac.uk; M.Fairweather@leeds.ac.uk

## **ABSTRACT**

Nucleate boiling is trusted as an efficient heat transfer mechanism in a wide range of engineering applications. However, the entire physical process of boiling is extremely difficult to predict with accuracy, and engineers have mostly relied on empirical models and correlations for this purpose. In recent years, however, significant advances in the development of more mechanistic approaches have been made. Developments are driven by the benefits in safety and efficiency that are achievable with a more accurate estimation of boiling heat transfer and a reduced operational safety margin on the critical heat flux. This paper further develops a bubble departure diameter mechanistic model based on the forces that impact bubble growth and departure. The heat transfer model includes contributions from the microlayer beneath the bubble, the superheated liquid layer around the bubble surface and condensation when the bubble cap is surrounded by subcooled liquid. Improvements in the modelling of the contribution of condensation are implemented and successfully tested. The model is validated against a large set of measurements that includes saturated and subcooled flow boiling and a new database for forced convection boiling in cross-flow conditions. This database is used to validate the model for the coupled calculation of bubble departure diameter and bubble departure frequency. Although the model predicts the bubble growth time with accuracy, improvements are still required in the modelling of the waiting time after bubble departure. Models of this kind can be used as a basis for the prediction of boiling beyond nucleate boiling conditions, as well as for implementation in wall boiling routines of computational fluid dynamic multiphase flow models.

## **KEYWORDS**

Nucleate boiling, departure diameter, departure frequency, subcooled boiling, bubble growth

## **1. INTRODUCTION**

Nucleate boiling is a very efficient heat transfer mechanism, employed in steam generators and boilers and in a vast number of applications in the energy field, including nuclear reactors. Saturated nucleate boiling cools boiling water reactors and transfers the thermal power from the core to the power cycle in the steam generator of pressurized water reactors (PWR). PWRs also often operate under local subcooling boiling conditions in the core. Boiling is also omnipresent in the specification of many design basis and beyond design basis postulated accident scenarios.

Despite its widespread application, nucleate boiling is still one of the most debated and active topics in nuclear thermal hydraulics [1]. After decades of continuous effort, a robust physical understanding of the complex mechanisms that govern nucleate boiling remains to be found [2] although, more recently, progress in experimental techniques [3,4] and detailed microscale

resolving computational fluid dynamic (CFD) simulations [5,6] have brought us closer to a comprehensive explanation. A consequence of this missing physical understanding has been that modelling efforts have for a long time being limited to mainly empirical treatments [7]. Only recently have more mechanistic methodologies based on first principles emerged, initiated by the well-known work of Klausner et al. [8]. In the latter model, the energy exchanged between the bubble and the surrounding fluid drives the growth of the bubble, and the balance of the forces exerted on the bubble surface its departure from the nucleation site.

This model has been progressively developed over the years, and is still today the basis of more mature and advanced methodologies [9-11]. Colombo and Fairweather [12] introduced the contribution of the microlayer underneath the bubble, the superheated liquid layer around the bubble surface and condensation on the bubble cap in the energy balance driving the growth. Gilman and Baglietto [13] extended the model from the isolated bubble regime towards higher heat fluxes and more sustained boiling conditions by accounting for static nucleation site interaction, dry surface area evolution and bubble sliding and merging on the heated surface. Ardron et al. [14] introduced a model based on thermodynamic equilibrium. In their model, validated against pool boiling data, the contact angle is identified as the most important parameter driving bubble departure at high pressure. Heat diffusion still drives the growth of the bubble, which departs when the contact angle approaches a zero value. The model was later extended to flow boiling conditions [15]. In the model of Ding et al. [16], the contact angle and the bubble base and shape are dynamically adjusted based on the instantaneous force balance. Bubbles depart forming a bottleneck and effective departure is achieved when this bottleneck breaks or the bottleneck base shrinks to zero. Despite ongoing efforts, however, greater accuracy and extended applicability are required, particularly when the model is applied over large ranges of flow conditions and liquid subcooling.

The continuous interest in these treatments is mainly aimed at implementation in wall boiling sub-models of CFD Eulerian-Eulerian two-fluid models [13,17-19]. These are mostly based on the well-known RPI heat flux partitioning approach [20], which mechanistically distributes the heat transfer between the mechanisms contributing to it, i.e. convection, evaporation and quenching. The evaporation contribution is then calculated from the number of active nucleation sites and the bubble departure diameter and frequency. The calculation of these terms, mainly because of the missing physical understanding, has for a long time been based on empirical closures that, neglecting any local flow and temperature effects, have proved to be largely inaccurate [21-23]. In this regard, the development of more mechanistic closures, such as for the bubble departure diameter, is currently viewed as one of the most promising ways towards improved CFD predictions of boiling flows.

Recent works have underlined the benefits of the coupled calculation of bubble departure diameter and frequency, not only for accuracy, but also for the internal consistency of CFD boiling models [17,24]. Conversely, the calculation of bubble departure diameter and frequency is uncoupled, and mutual relations between these two parameters are largely ignored. In this work, we have extended our existing model [12] for the prediction of bubble departure diameter to the coupled calculation of departure diameter and frequency, comparing predictions against a recently published database of saturated flow boiling that provides measurements of both parameters [25]. In contrast, validation of models has been normally limited to the bubble departure diameter alone in most literature studies [10,12,15,26]. The database was obtained in a horizontal rod bundle in crossflow and, therefore, provides also the opportunity to test the model in more challenging conditions than found in the more commonly used validation datasets. Comparison with data is also extended to two additional saturated boiling databases [8,27], extending the validation of the model performed in the past. In the final part of this work, a more consistent and improved modelling of the condensation on the bubble cap is evaluated against three databases on subcooled boiling flows [9,10,28]. Overall, the work described is aimed at improving the modelling of bubble diameter and

frequency through a modelling approach suitable for implementation in CFD two-fluid boiling models.

## 2. MATHEMATICAL MODEL

The departure of a bubble is evaluated from the balance of the forces that act on the bubble surface while it grows, attached to the nucleation site. In the direction parallel (x-direction) and perpendicular (y-direction) to the heating surface, these balances are:

$$\sum F_x = F_{stx} + F_{qsd} + F_b \sin \theta + F_{udx} = 0 \quad (1)$$

$$\sum F_y = F_{sty} + F_{sl} + F_b \cos \theta + F_{udy} + F_p + F_{cp} = 0 \quad (2)$$

In the above equations,  $F_{st}$  is the surface tension force,  $F_{qsd}$  the quasi-steady drag force,  $F_b$  the buoyancy force,  $F_{sl}$  the shear lift force,  $F_{ud}$  the unsteady drag force due to asymmetrical bubble growth,  $F_p$  the force due to hydrodynamic pressure and  $F_{cp}$  the contact pressure force. Subscripts x and y refer to the component of the forces (when applicable) acting in the x and y directions, respectively. A graphical representation of all the acting forces is provided in Figure 1 and a summary in Table I. Detachment of the bubble from the nucleation site occurs when Eq. (1) or Eq. (2) is violated and the detaching forces (mainly buoyancy, drag and shear lift) overcome the forces that keep the bubble attached to the surface (mainly surface tension and bubble growth). If the balance in the x-direction is violated first, the bubble departs from the nucleation site and starts sliding along the heated surface until it lifts off into the liquid stream. The diameter at which the x-direction balance is violated identifies the bubble departure diameter. Conversely, the bubble lifts off from the wall without sliding if Eq. (2) is violated first. In this case, the diameter at which the y-direction balance is violated identifies the bubble departure diameter which coincides with the lift-off diameter.

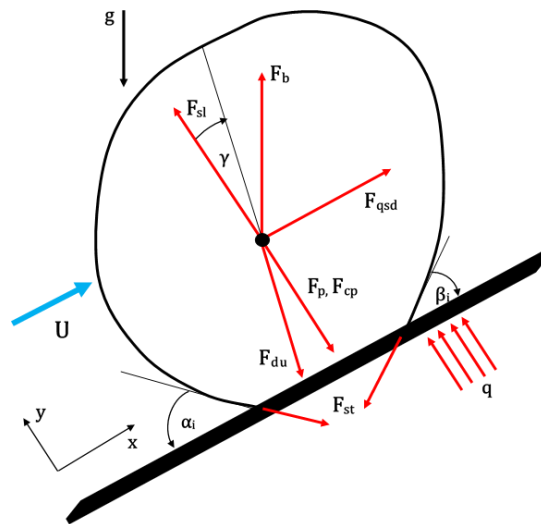


Figure 1. Schematic of the forces acting on a bubble growing at a nucleation site [12].

In the formula of the forces, the most uncertain parameters are the advancing contact angle,  $\alpha_i$ , and the receding contact angle,  $\beta_i$ , in addition to the contact diameter between the bubble and the heated surface,  $d_w$ . Measurements and reliable models for these parameters are not common in the literature, although models of the kind described have proved to be quite sensitive to these values. Here, we have used the values recommended in Klausner et al. [8] for the contact angles and the model proposed by Yun et al. [19] for the contact diameter. In this approach, the ratio between the contact diameter and the bubble diameter is assumed to

be constant and equal to 1/15. Different values were only used for the Sugrue and Buongiorno [10] subcooled boiling database in the second part of the paper, in view of the good agreement reported by the authors with the contact angles they measured and a different ratio of the contact to bubble diameter.

Prior to departure, only the asymptotic phase of the bubble growth, governed by the diffusion of heat from the surrounding liquid, is considered and bubbles are assumed hemispherical during their growth. The present model includes the evaporation of the thin liquid micro-layer formed under the bubble during its growth, heat diffusion from the superheated layer around the bubble surface and, eventually in subcooled boiling, condensation on the bubble cap. Micro-layer evaporation is modelled as in Cooper and Loyd [29], with the superheated contribution from Plesset and Zwick [30] and condensation on the bubble cap from the Ranz and Marshall correlation [31]:

$$\frac{dr(t)}{dt} = \frac{1}{C_2} Pr^{-0.5} Ja \alpha^{0.5} t^{-0.5} + \sqrt{\frac{3}{\pi}} Ja \alpha^{0.5} (1-b) t^{-0.5} - \frac{h_c}{\rho_v l_{lv}} (T_{sat} - T_{sub}) b \quad (3)$$

The parameter  $b$  determines the portion of the bubble surface in contact with subcooled liquid. To determine this, knowledge of the temperature profile in the boundary layer is required, but this is not easy to determine. In addition to this, the wall temperature is not always available from experiments. To overcome these issues, we have applied the following procedure. If not available, the wall temperature is calculated from the correlation of Chen [32]. Then, the temperature profile of a single-phase flow under the same conditions of flow rate and heat flux is calculated from the wall function of Kader [33]. The two-phase flow profile is assumed to have the same shape, with a value scaled with the ratio of the two-phase to single-phase wall superheating  $R = (T_w - T_{sat}) / (T_{w,SP} - T_{sat})$ :

$$T_y = T_{sat} + (T_{y,SP} - T_{sat}) \cdot R \quad (4)$$

When the temperature becomes lower than saturation, the single-phase profile is assumed. From knowledge of the temperature difference, the location of the saturation temperature and the temperature on the cap of the bubble are then found. In the subcooled region, the effective temperature ( $T_{sub}$  in Eq. (3)) is taken as the average between the saturation and the cap values. In the superheated region, the average between the saturation and wall temperatures is used ( $T$  in Eq. (3)). Obviously, until the cap is in the superheated region, condensation is neglected. In our previous model, it was necessary to include a limiter equal to 0.5 on the parameter  $b$ , to avoid excessive condensation [12]. With the procedure employed here for the calculation of temperature, the limiter is no longer necessary.

Once bubble departure is detected, the time at departure is recorded and this is equated to the bubble growth time,  $t_G$ . A full bubble ebullition cycle is the sum of this growth time and the waiting time, during which the wall temperature and the thermal boundary layer recover after being perturbed by the departure of the previous bubble and the liquid superheat returns to a level sufficient to allow the nucleation of the next bubble. In view of the importance of the waiting phase, some recent models have incorporated it directly through a heat balance on the heating surface [16,34]. Here, we use the commonly employed approach in the context of CFD two-fluid models of assuming the waiting time equal to 80% of the entire ebullition cycle. With this assumption, the bubble departure frequency can be calculated as follows:

$$f_D = \frac{0.2}{t_G} \quad (5)$$

The overall model was implemented in MATLAB [35]. At each time step, the model is advanced in time using a forward method. Eq. (3) is integrated by assuming that temperature and fluid properties remain constant and equal to their values at the previous time step. Once the value of the radius at the new time-step is known, the force balances are evaluated (Eq. (1) and Eq. (2)). If the balances are not violated, the calculation continues. If Eq. (1) is violated first, the current diameter is taken as the value at departure and the calculation is carried on neglecting the contact diameter between the bubble and the heated surface (therefore the surface tension forces). Bubble lift-off is then obtained when Eq. (2) is also violated. If Eq. (2) is violated first, the bubble directly lifts off from the nucleation site and the bubble departure and lift off diameter coincide.

For validation of the model, measurements from six databases are used in the following section, including the new measurements recorded by Goel et al. [25] at the Bhabha Atomic Research Centre in a horizontal rod bundle under crossflow of water at saturation temperature and atmospheric pressure. For this database, values of bubble departure diameter and frequency are available and this allows the coupled validation of the model. In addition, five other databases are considered, which are amongst the most frequently used for validation of this type of model. These comprise the saturated boiling databases in refrigerant R113 of Klaunser et al [8] and Zeng et al [27] and the subcooled boiling databases of Sugrue and Buongiorno [10], Prodanovic et al. [28] and Situ et al. [9] for the subcooled boiling of water.

Table I. Summary of the model for bubble departure diameter and bubble departure frequency.

Model	Form
<b>Bubble Departure Diameter</b>	
Force balance	$F_{stx} = -1.25d_w\sigma \frac{\pi(\alpha_i - \beta_i)}{\pi^2 - (\alpha_i - \beta_i)^2} (\sin \alpha_i - \sin \beta_i)$ $F_{sty} = -d_w\sigma \frac{\pi}{(\alpha_i - \beta_i)} (\cos \beta_i - \cos \alpha_i)$ $F_{qsd} = 6\pi\rho_l\nu Ur \left\{ \frac{2}{3} + \left[ \left( \frac{12}{Re} \right)^{0.65} + 0.862 \right]^{-1.54} \right\}$ $F_{du} = -\rho_l\pi r^2 \left( \frac{3}{2}\dot{r}^2 - r\ddot{r}^2 \right)$ $F_b = \frac{4}{3}\pi r^3(\rho_l - \rho_v)g$ $F_{sl} = \frac{1}{2}\pi\rho_l U^2 r^2 \{ 3.877G_s^{0.5} [Re^{-2} + (0.344G_s^{0.5})^4]^{0.25} \}$ $F_p = \frac{9}{8}\rho_l U^2 \frac{\pi d_w^2}{4}$ $F_{cp} = \frac{\sigma \pi d_w^2}{r \cdot 4}$

Bubble Departure Frequency	
Frequency	$f_D = \frac{1}{t_G + t_w} = \frac{0.2}{t_G}$
Waiting time	$t_w = \frac{0.8}{f_D}$

### 3. RESULTS AND DISCUSSION

#### 3.1 Bubble departure diameter, frequency and bubble growth in saturated boiling

The model is first applied to the Goel et al. [25] database in a horizontal rod bundle under saturated conditions (Figure 2). Comparison for saturated boiling also given with the data of Klaunser et al. [8] and Zeng et al. [27] with refrigerant R113 (Figure 3). The data of Zeng et al. [27] extends the number of databases the model has been compared against in the past. Overall, satisfactory accuracy is found. The data from Kalunser et al. [8] and Zeng et al. [27] are well-predicted, with most of the predictions included in the range  $\pm 30\%$  and with average errors around 20%. Larger discrepancies are found for the data of Goel et al. [25], as might have been expected. These data were obtained on a single horizontal cylindrical rod and in a horizontal rod bundle, with the number of active rods changed between experiments. Therefore, some of the data were obtained in temperature and flow conditions that are difficult to replicate in the present model. However, the model still maintains a reasonable accuracy and generally good applicability and, except for a few data points at high diameter, provides reliable predictions even in under these challenging conditions. The worst accuracy is found for a series of data that show values of the bubble diameter up to 4 mm and which were measured in conditions which represent the most challenging to predict, with the heated rod in the middle of the rod bundle and with two other rods simultaneously active.

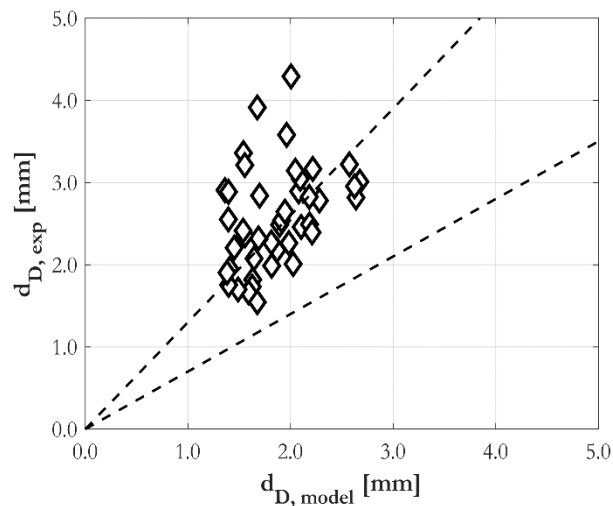


Figure 2. Bubble departure diameter predictions compared with the data of Goel et al. [25]; (---)  $\pm 30\%$  range.

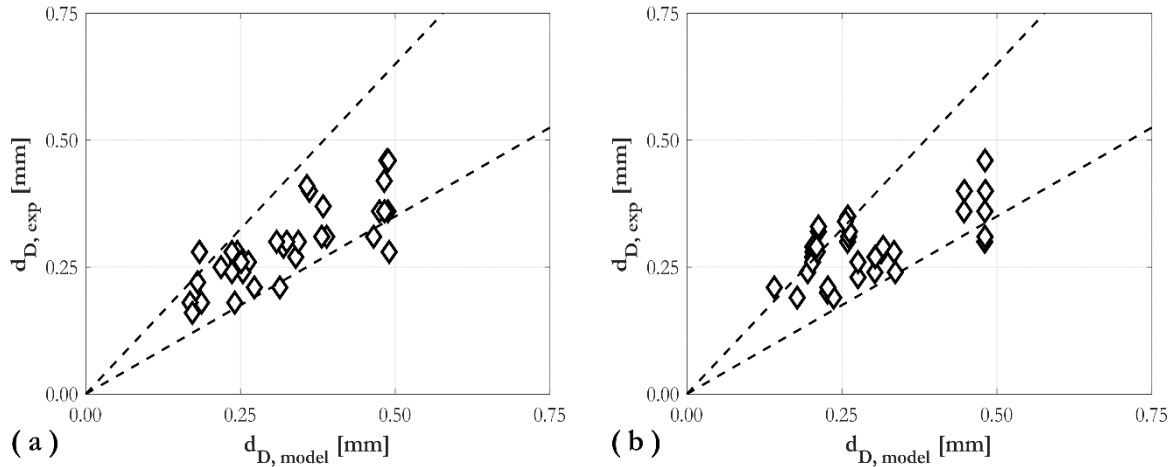


Figure 3. Bubble departure diameter predictions compared with data of: (a) Klausner et al. [8]; (b) Zeng et al. [27]; (---)  $\pm 30\%$  range.

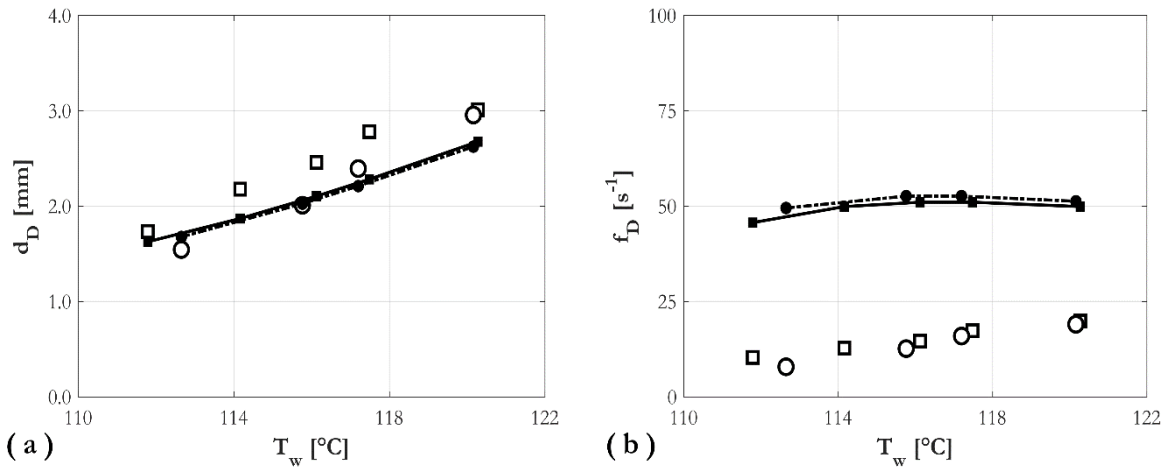


Figure 4. Model predictions against the data of Goel et al. [25] for a single horizontal cylindrical rod: (a) bubble departure diameter; (b) bubble departure frequency. ( $\square$ , —)  $G = 81.3 \text{ kg m}^{-2} \text{ s}^{-1}$ ; ( $\circ$ , - · -)  $G = 147.8 \text{ kg m}^{-2} \text{ s}^{-1}$ .

The data of Goel et al. [25], as mentioned before, include measurements of both the bubble departure diameter and the bubble departure frequency. A selection of these data is shown in Figure 4, where both the departure diameter and frequency are provided as a function of the wall superheat for a single horizontal rod and two different mass fluxes. The bubble departure diameter in Figure 4(a) is well-predicted for both mass fluxes. At the lower mass flux, the bubble departure diameter is higher because of the reduced action of the fluid (through drag and shear lift forces) that tends to strip the bubbles from the nucleation site. This effect is not, however, a major factor in the experiments, since the two mass fluxes are close to one another and relatively low. This effect is even less pronounced in the predictions of the model, where bubble departure diameters at the two mass fluxes are only very slightly different. With an increase of the wall temperature, additional energy flows into the bubble from the outside liquid and bubble growth is more sustained. Therefore, the growth force, induced by the inertia of the surrounding liquid which keeps the bubble attached to the nucleation site, is higher and allows the bubble to grow more before departure. This effect is well-predicted by the model, and the bubble departure diameter increases with the wall temperature for sets of predictions.

Despite the good predictions of the bubble departure diameter, the departure frequency is not predicted with any degree of accuracy, and values more than double those of the experiments are found in Figure 4(b). With regards to qualitative trends, no significant effect of the mass

flux is found, in both the experiments and simulations. On the other hand, the frequency increases slightly with the wall temperature, as a consequence of the faster growth of the bubbles, although this effect is not captured by the model.

Two additional sets of data are shown in Figure 5, for a single heated rod but this time in the middle of a rod bundle, and two more different mass flow rates. Bubble departure diameter predictions are not as good as those in Figure 4(a), but maintain a reasonable accuracy (Figure 5(a)). The effect of the mass flow rate is well-predicted, with differences between the predictions that match the difference between the two sets of experimental measurements. A reduction in quantitative accuracy is probably related to the rod being in a rod bundle. There, the rod is hidden to the flow by the surrounding rods, and the flow effect on the bubble is therefore likely reduced. This effect cannot be captured by the model, which therefore predicts a lower departure diameter, as if the bubbles were in an undisturbed flow.

Predictions of the bubble departure frequency (Figure 5(b)), although still not satisfactory, are improved with respect to those of Figure 4(b). Specifically, the bubble departure frequency is less underestimated, in particular at the lowest mass flow rate. However, the model predictions look similar to those of Figure 4(b), whilst the experimental measurements are significantly higher. This can be again explained by the heated rod being inside the bundle. Once a bubble departs, the thermal boundary layer needs to reform, with this period of time during the bubble ebullition cycle known as the waiting time. Being less disturbed by the flow inside the bundle, the thermal boundary layer can therefore reform in much less time, resulting in a much higher departure frequency. This role of the waiting time suggests an additional comparison, since some data are also available for the bubble growth time alone. Therefore, model predictions of the growth time are shown in Figure 6. Growth times are provide for typical conditions by Goel et al. [25], therefore we have compared these with our predictions at the same thermal power but at different mass fluxes.

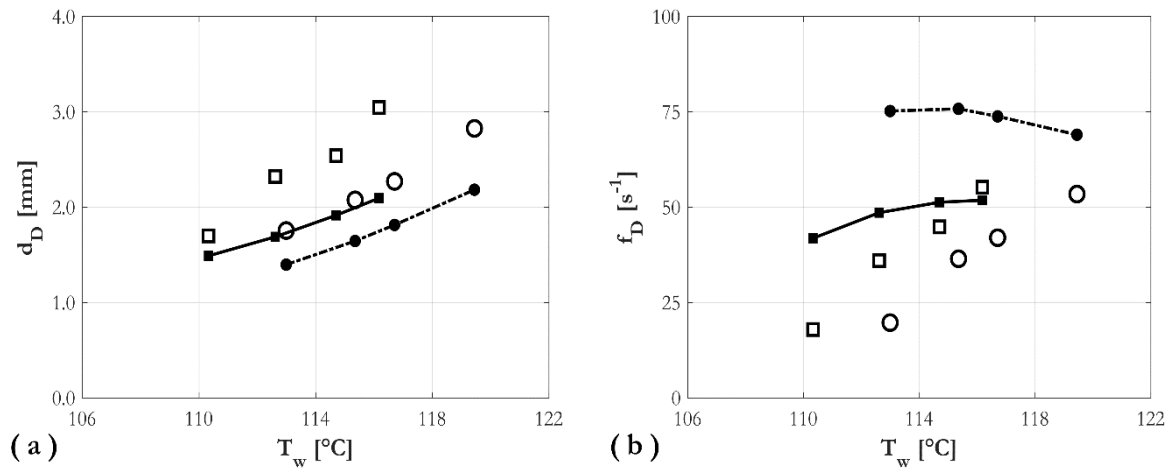


Figure 5. Model predictions against the data of Goel et al. [25] for a cylindrical rod in a horizontal rod bundle: (a) bubble departure diameter; (b) bubble departure frequency. ( $\square, \text{—}$ )  $G = 121.4 \text{ kg m}^{-2} \text{ s}^{-1}$ ; ( $\circ, - \cdot -$ )  $G = 303.5 \text{ kg m}^{-2} \text{ s}^{-1}$ .

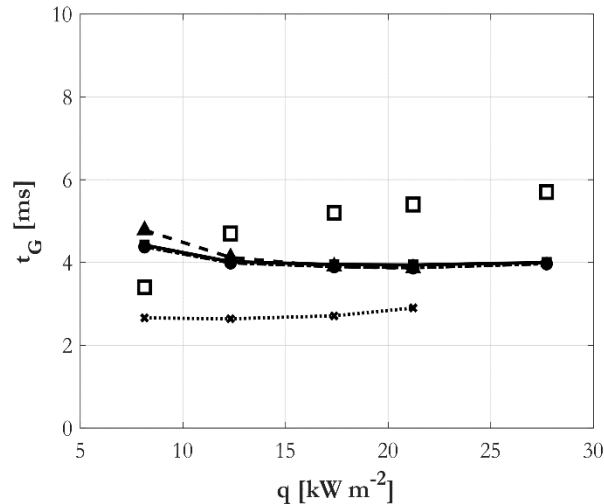


Figure 6. Model predictions of bubble growth time against the data of Goel et al. [25] at different wall heat flux: ( $\square$ ) data; ( $—$ ) single rod,  $G = 59.1 \text{ kg m}^{-2} \text{ s}^{-1}$ ; ( $- \cdot -$ ) single rod  $G = 81.3 \text{ kg m}^{-2} \text{ s}^{-1}$ ; ( $---$ ) rod bundle,  $G = 121.4 \text{ kg m}^{-2} \text{ s}^{-1}$ ; ( $\cdots$ ) rod bundle,  $G = 303.5 \text{ kg m}^{-2} \text{ s}^{-1}$ .

In Figure 6, the predicted growth time of the bubbles is much more consistent with experiment, and their accuracy can be considered satisfactory. The main difference is still the fact that the measured growth time slightly increases with the heat flux, while the model predictions remain essentially flat. Larger discrepancies were found in the rod bundle at the highest mass flow rate, which are the most difficult to predict considering the present capabilities of the model. Disturbances to the flow, and temperature, fields are not accounted for in the model, and the growth time and the bubble diameter are consequently under-predicted because of the excessive influence of the fluid flow field. Overall, and in view of the ability of the model to predict the growth time, in future works we will focus our attention on modelling of the waiting time and the reforming of the thermal boundary layer which are currently taken into account in a very simplistic fashion.

### 3.2. Bubble departure diameter in subcooled boiling

Lastly, and in view of the improved procedure to evaluate the temperature profile and the impact of liquid subcooling, the model is re-evaluated against the three databases on subcooled boiling already used in [12]. Overall results are provided in Figure 7. Generally, subcooled conditions are more difficult to predict because of the additional effects of condensation that induce higher uncertainty. However, the reformulated model shows good applicability and promising results, although further improvements are necessary as condensation is still evaluated from the Ranz and Marshall [31] correlation, and due to the many uncertainties that still affect the temperature profile around the bubble. Overall, the model's accuracy is in line with other literature works that have predicted the same subcooled boiling databases [15,26].

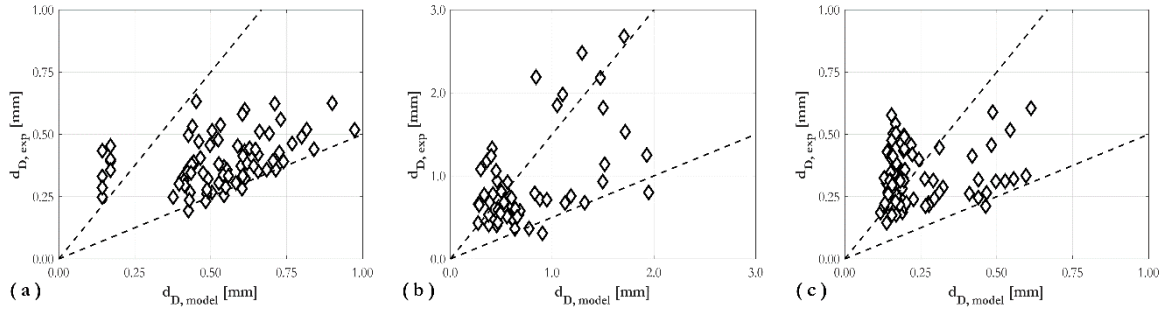


Figure 7. Model predictions of bubble departure diameter compared with experimental measurements in subcooled boiling conditions: (a) Sugrue and Boungiorno [10]; (b) Prodanovic et al. [28]; (c) Situ et al. [9]; (---)  $\pm 50\%$  range.

## 4. CONCLUSIONS

A model for the calculation of bubble departure diameter has been validated against saturated and subcooled flow boiling data. In addition, predictions of the bubble departure frequency from the same model were also evaluated using a new set of data providing measurements of both bubble departure diameter and frequency. The model shows good accuracy in saturated boiling, and even in horizontal rod bundles, where the impact of temperature and velocity fields on bubble departure are more difficult to model precisely. In subcooled boiling, an improved procedure for the evaluation of the liquid temperature distribution around the bubble surface has improved the generality of the model. With regards to accuracy, this is in line with other available models that have been evaluated using the same databases.

Analysis of the bubble departure frequency predictions revealed that the growth time is well-predicted by the model, although the waiting time, inaccurately modelled as the 80 % of the total ebullition cycle, compromises the accuracy of the frequency calculation. Future developments will therefore prioritize this aspect of the model, and this is already the focus of ongoing research. In other areas, further improvements will be required in the subcooling calculation and the modelling of contact angles, dry area under the bubble and contact area between the bubble and the heating surface.

## NOMENCLATURE

$b$	fraction of the bubble in contact with subcooled liquid [-]
$C_p$	specific heat at constant pressure [ $\text{J kg}^{-1} \text{K}^{-1}$ ]
$D$	pipe diameter [m]
$d_D$	bubble departure diameter [m]
$d_w$	contact diameter [m]
$F$	force [N]
$f_D$	bubble departure frequency [ $\text{s}^{-1}$ ]
$G$	mass flux [ $\text{kg m}^{-2} \text{s}^{-1}$ ]
$G_s$	dimensionless shear rate [-]
$g$	gravitational acceleration [ $\text{m s}^{-2}$ ]
$hc$	condensation heat transfer coefficient [ $\text{W m}^{-2}\text{K}^{-1}$ ]
$i_{lv}$	latent heat of vaporization [ $\text{J kg}^{-1}$ ]
$Ja$	Jacob number $Ja = \rho_l C_{p,l} (T - T_{sat}) / (\rho_v i_{lv})$ [-]
$Pr$	Prandtl Number [-]
$q$	thermal flux [ $\text{W m}^{-2}$ ]
$r$	bubble radius [m]
$Re$	bubble Reynolds number [-]
$T$	temperature [K]
$t$	time [s]

$t_g$	growth time [s]
$t_w$	waiting time [s]
$U$	velocity [ $\text{m s}^{-1}$ ]

### **Greek symbols**

$\alpha$	thermal diffusivity [-]
$\alpha_i$	advancing contact angle [rad]
$\beta_i$	receding contact angle [rad]
$\gamma$	bubble inclination angle [rad]
$\theta$	heated surface inclination angle [rad]
$\nu$	kinematic viscosity [ $\text{m}^2 \text{s}^{-1}$ ]
$\rho$	density [ $\text{kg m}^{-3}$ ]
$\sigma$	surface tension [ $\text{N m}^{-1}$ ]

### **Subscripts**

b	buoyancy
cp	contact pressure
du	unsteady drag
exp	experimental results
l	liquid
model	model results
p	pressure
qsd	quasi-steady drag
sat	saturation
sl	shear lift
SP	single-phase
st	surface tension
sub	subcooled
v	vapour
y	normal distance from the wall
w	wall

## **ACKNOWLEDGEMENTS**

The University of Leeds gratefully acknowledges the financial support of the EPSRC under grants EP/M018733/1, Grace Time, and EP/R021805/1, Development and Validation of Thermal-Hydraulic Prediction Methods for Licensing, Fault Conditions and Severe Accidents in BWRs and PWRs.

## **REFERENCES**

1. G. Yadigaroglu, "CMFD and the critical-heat-flux grand challenge in nuclear thermal-hydraulics", *International Journal of Multiphase Flow*, **67**, pp. 3-12 (2014).
2. G. Liang, I. Mudawar, "Pool boiling critical heat flux (CHF) - Part 1: Review of mechanisms, models and correlations", *International Journal of Heat and Mass Transfer*, **117**, pp. 1352-1367 (2018).
3. S. Jung, H. Kim, "Observation of the mechanism triggering critical heat flux in pool boiling of saturated water under atmospheric pressure", *International Journal of Heat and Mass Transfer*, **128**, pp. 229-238 (2019).
4. A. Richenderfer, A. Kossolapov, J.H. Seong, G. Saccone, E. Demarly, R. Kommajosyula, E. Baglietto, J. Buongiorno, M. Bucci, "Investigation of subcooled flow boiling and CHF using high-resolution diagnostics", *Experimental Thermal and Fluid Science*, **99**, pp. 35-58 (2018).

5. S. Hänsch, S. Walker, "Microlayer formation and depletion beneath growing steam bubbles", *International Journal of Multiphase Flow*, **111**, pp. 241-263 (2019).
6. Y. Sato, B. Niceno, "Pool boiling simulation using an interface tracking method: from nucleate boiling to film boiling regime through critical heat flux", *International Journal of Heat and Mass Transfer*, **125**, pp. 876-890 (2018).
7. R.L. Mohanty, M.K. Das, "A critical review on bubble dynamics parameters influencing boiling heat transfer", *Renewable and Sustainable Energy Reviews*, **78**, pp. 466-494 (2017).
8. J.F. Klausner, R. Mei, D.M. Bernhard, L.Z. Zeng, "Vapor bubble departure in forced convection boiling", *International Journal of Heat and Mass Transfer*, **36**, pp. 651-662 (1993).
9. R. Situ, T. Hibiki, M. Ishii, M. Mori, "Bubble lift-off size in forced convective subcooled boiling flow", *International Journal of Heat and Mass Transfer*, **48**, pp. 5536-5548 (2005).
10. R. Sugrue, J. Buongiorno, "A modified force-balance model for prediction of bubble departure diameter in subcooled flow boiling", *Nuclear Engineering and Design*, **305**, pp. 717-722 (2016).
11. W. Wu, P. Chen, B.G. Jones, T.A. Newell, "A study of bubble detachment and the impact of the heated surface structure in subcooled nucleate boiling flows", *Nuclear Engineering and Design*, **238**, pp. 2693-2698 (2008).
12. M. Colombo, M. Fairweather, "Prediction of bubble departure in forced convection boiling: A mechanistic model", *International Journal of Heat and Mass Transfer*, **85**, pp. 135-146 (2015).
13. L. Gilman, E. Baglietto, "A self-consistent, physics-based boiling heat transfer modeling framework for use in computational fluid dynamics", *International Journal of Multiphase Flow*, **95**, pp. 35-53 (2017).
14. K.H. Ardron, G. Giustini, S.P. Walker, "Prediction of dynamic contact angles and bubble departure diameters in pool boiling using equilibrium thermodynamics", *International Journal of Heat and Mass Transfer*, **114**, pp. 1274-1294 (2017).
15. G. Giustini, K.H. Ardron, S.P. Walker, "Modelling of bubble departure in flow boiling using equilibrium thermodynamics", *International Journal of Heat and Mass Transfer*, **122**, pp. 1085-1092 (2018).
16. W. Ding, E. Krepper, U. Hampel, "Evaluation of the microlayer contribution to bubble growth in horizontal pool boiling with a mechanistic model that considers dynamic contact angle and base expansion", *International Journal of Heat and Fluid Flow*, **72**, pp. 274-287 (2018).
17. M. Colombo, R. Thakrar, M. Fairweather, S.P. Walker, "Assessment of semi-mechanistic bubble departure diameter modelling for the CFD simulation of boiling flows", *Nuclear Engineering and Design*, **344**, pp. 15-27 (2019).
18. G.H. Yeoh, S. Vahaji, S.C.P. Cheung, J.Y. Tu, "Modeling subcooled flow boiling in vertical channels at low pressures - Part 2: Evaluation of mechanistic approach", *International Journal of Heat and Mass Transfer*, **75**, pp. 754-768 (2014).
19. B.J. Yun, A. Splawski, S. Lo, C.H. Song, "Prediction of a subcooled boiling flow with advanced two-phase flow models", *Nuclear Engineering and Design*, **253**, pp. 351-359 (2012).
20. N. Kurul, M.Z. Podowski, 1990. Multi-dimensional effects in sub-cooled boiling. 9<sup>th</sup> International Heat Transfer Conference, Jerusalem, Israel, August 19-24.
21. S.C.P. Cheung, S. Vahaji, G.H. Yeoh, J.Y. Tu, "Modeling subcooled flow boiling in vertical channels at low pressures - Part 1: Assessment of empirical correlations", *International Journal of Heat and Mass Transfer*, **75**, pp. 736-753 (2014).
22. M. Colombo, M. Fairweather, "Accuracy of Eulerian-Eulerian, two-fluid CFD boiling models of subcooled boiling flows", *International Journal of Heat and Mass Transfer*, **103**, pp. 28-44 (2016).
23. R. Thakrar, J. Murallidharan, S.P. Walker, 2014. An evaluation of the RPI model for the prediction of the wall heat flux partitioning in subcooled boiling flows. 22<sup>nd</sup> International Conference on Nuclear Engineering (ICONE-22), Prague, Czech Republic, July 7-11.

24. R. Thakrar, S.P. Walker, 2016. CFD prediction of subcooled boiling flow with semi-mechanistic bubble departure diameter modelling. 25<sup>th</sup> International Conference Nuclear Energy for New Europe (NENE-2016), Portoroz, Slovenia, September 5-8.
25. P. Goel, A.K. Nayak, M.K. Das, J.B. Joshi, "Bubble departure characteristics in a horizontal tube bundle under cross flow conditions", *International Journal of Multiphase Flow*, **100**, pp. 143-154 (2018).
26. T. Mazzocco, W. Ambrosini, R. Kommajosyula, E. Baglietto, "A reassessed model for mechanistic prediction of bubble departure and lift off diameters", *International Journal of Heat and Mass Transfer*, **117**, pp. 119-124 (2018).
27. L.Z. Zeng, J.F. Klausner, R. Mei, "A unified model for the prediction of bubble detachment diameters in boiling systems- II. Flow boiling", *International Journal of Heat and Mass Transfer*, **36**, pp. 2271-2279 (1993).
28. V. Prodanovic, D. Fraser, M. Salcudean, "Bubble behaviour in subcooled flow boiling of water at low pressures and low flow rates", *International Journal of Multiphase Flow*, **28**, pp. 1-19 (2002).
29. M.G. Cooper, A.J.P. Lloyd, "The microlayer in nucleate pool boiling", *International Journal of Heat and Mass Transfer*, **12**, pp. 895-913 (1969).
30. M.S. Plesset, S.A. Zwick, "The growth of vapor bubbles in superheated liquids", *Journal of Applied Physics*, **25**, pp. 493-500 (1954).
31. W.E. Ranz, W.R. Marshall, "Evaporation from drops", *Chemical Engineering Progress*, **48**, pp. 141-146 (1952).
32. J.C. Chen, "Correlation for boiling heat transfer to saturated fluids in convective flow", *Industrial & Engineering Chemistry Research*, **5**, pp. 322-329 (1966).
33. B.A. Kader, "Temperature and concentration profiles in fully turbulent boundary layers", *International Journal of Heat and Mass Transfer*, **24**, pp. 1541-1544 (1981).
34. Z. Wang, M.Z. Podowski, "Analytical model of the effect of heater geometry on boiling heat transfer", *Nuclear Engineering and Design*, **344**, pp. 122-130 (2019).
35. MATLAB 2018a. The MathWorks, Inc., Natick, Massachusetts, United States.